Study of Superconductivity and Ferromagnetism Coexistence using Polarized Neutron Reflectometry

Author: Student Reiner Ramos Blazquez

Supervisor's name: Mrs. Vladimir. D. Zhaketov

Joint Institute for Nuclear Research

Final Report on the Interest Programme

Introduction

Artificial heterostructures with alternating superconducting (S) and ferromagnetic (F) layers are currently attracting great attention due to a diverse set of proximity effects.

The proximity phenomena in condensed matter physics are known to include the interface effects, which are usually associated with the exchange of electrons between the contacting materials. Such electromagnetic proximity effect can strongly affect the physics of superconductor-ferromagnet (SF) systems [1].

Let's consider a bilayer system consisting of a superconducting (S) film placed in contact with a ferromagnetic (F) layer with the magnetic moment parallel to the layer plane (Fig. 1). Considering the S and F subsystems to be isolated, we get a perfect example of complete separation of the regions with a nonzero concentration of Cooper pairs and magnetic field. The latter is completely trapped inside the ferromagnet. As we allow the electron transfer between the subsystems, the Cooper pairs immediately penetrate the ferromagnet inducing pair electron correlations there. This process which is usually referred to as a standard proximity effect leads to a series of fascinating transport phenomena. The inverse proximity effect, namely, the transfer of the magnetic moment from the ferromagnetic to the superconducting subsystem is also possible. This inverse proximity effect is related to the spin polarization of electrons forming the Cooper pair near the S/F interface (Fig.2) and results in the small magnetization of the superconducting surface layer at the depth of the order of the Cooper pair size ξ_S~1–10nm.

Considering a bilayer consisting of a superconductor of thickness $d_S >> \lambda$ and a ferromagnet of thickness $d_F << \lambda$ with the uniform magnetization $\mathbf{M_0} = M_0\mathbf{e_z}$. the magnetic field induced in the superconductor is $B_z = -4\pi M_0 Q \exp(x/\lambda_0)$, where $Q=\int_0^{d_F} \lambda^{-2}(x')x'dx'$. In the conventional regime, when the superconducting condensate penetrating the F layer reveals a diamagnetic response with Q>0, the magnetic field induced in the S layer is anti-parallel to the magnetization $\mathbf{M_0}$.

In the case where d_F is of the order of the superconducting coherence length in the ferromagnet ξ_F, the basic estimate gives $Q \sim (\xi_F/\lambda)^2 \sim 10^{-2}$ for the S/F structures based, e.g., on thin Nb films. Considering the experiments probing the change in the magnetic moment in SF structures when cooling down through the superconducting critical temperature and taking the typical magnetization corresponding to Fe or Co films $4\pi M_0 \sim 10^4$ Oe, we find $B_z \sim 10^2$ Oe, which is an easily measurable value.

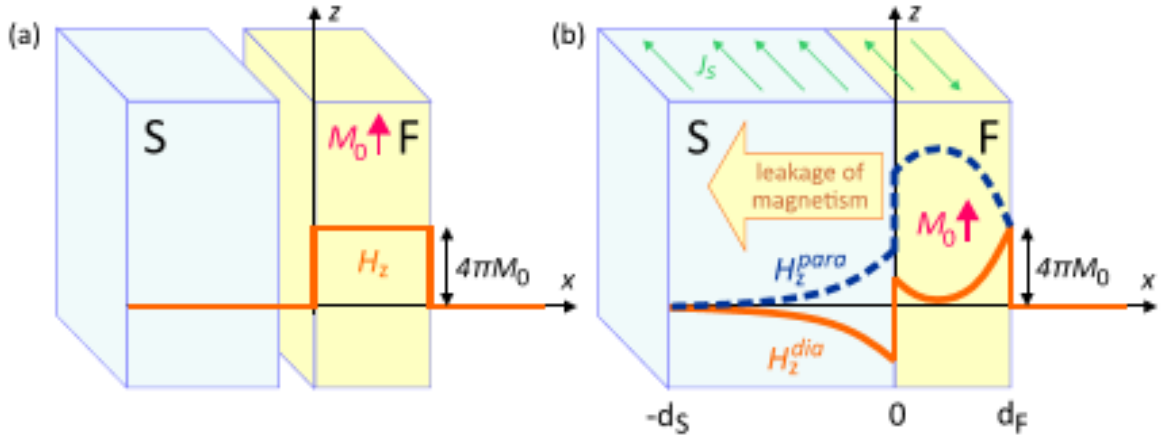

Fig.1. The sketch of the superconductor/ferromagnet bilayer. (a) When the layers are separated from each other, the magnetic field exists only inside the F layer. (b) In contrast, when the layers are put in contact, the magnetization inside the ferromagnet becomes the source of the long-range magnetic field in the superconductor. In both panels, the orange solid (blue dashed) curves schematically represent the profile of the magnetic field when the total current inside the F-layer is diamagnetic (paramagnetic).

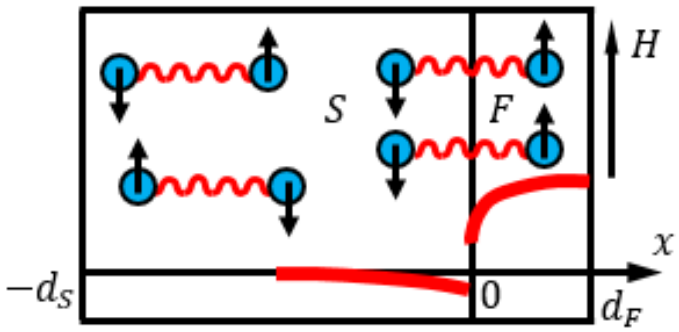

Fig.2. Spin polarization of electrons forming the Cooper pair near the S/F interface.

The magnetic field in the S layer can be substantially increased provided the magnetization in the F layer has a non-collinear structure. To illustrate the origin of this effect, let us assume that the ferromagnet consists of two layers: one layer F_1 occupying the region $0<x<d_1$ has magnetization M_0 along the z-axis, while

another layer F_2 of thickness d_2 has the same magnetization M_0 but directed along the y-axis (see Fig.3).

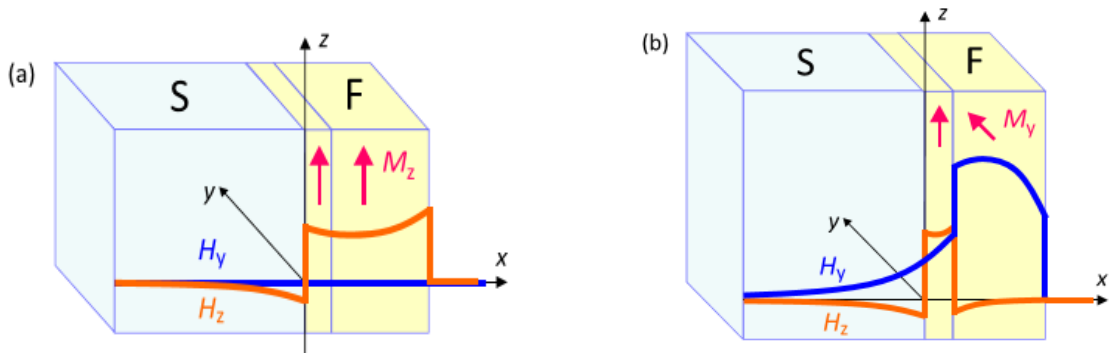

FIG.3. The profiles of the spontaneous magnetic field in the superconductor-ferromagnet-ferromagnet trilayer when the magnetic moments in the two F layers are (a) parallel to each other and (b) perpendicular to each other.

Let us analize two different structures. The first one: superlattices of composition $[Gd(d_F)/Nb(25\ nm)]_{12}$ deposited on Al_2O_3 substrates and covered by a Nb capping layer [2]. There were created different configurations that are described in three different samples. The thickness of the Gd layers was chosen to be $d_F=0.5\xi_F$ (sample 1), $0.75\xi_F$ (sample 2), and $1.25\,\xi_F$ (sample 3). Experimental measurements showed a suppression of the spin asymmetry of the first Bragg peak below Tc after zero-field cooling. The effect takes place in an intermediate range of magnetic fields between remanesce and saturation. Owing to the proximity effect the entire Gd/Nb superlattice behaves as a uniform thick (magnetic) superconductor $D_S=12D\approx300$ nm. As a thick superconductor it is able to screen the applied magnetic field, thus suppressing the ferromagnetic response of the inner Gd layers. This effect is to some extent similar to the cryptoferromagnetism. In analogy to CFM, it leads to a transition from homogeneous magnetic order above Tc to inhomogeneous order (along z in our case) below Tc, and hence to a suppression of the averaged magnetic moment. Similar to CFM, the effect takes place for a weakened ferromagnet ($d_F<\xi_F$) and strengthened superconductor ($D_S>\lambda$).

For the experimental investigation of the inverse proximity effects in structure V (40 nm)/Fe (1 nm) in [3] different magnetometric methods have been used. The SQUID magnetometer was used to define the temperature dependence of the magnetic moment in the vicinity of the superconducting phase transition (Fig. 4(a)). Before the cooling the F layer was saturated in a magnetic field H = 1 kG and then cooled down below Tc in a magnetic field H = 10 Oe. The measurement has shown that below Tc a 40% increase in the magnetic moment takes place, which is consistent with the waveguide enhanced PNR data.

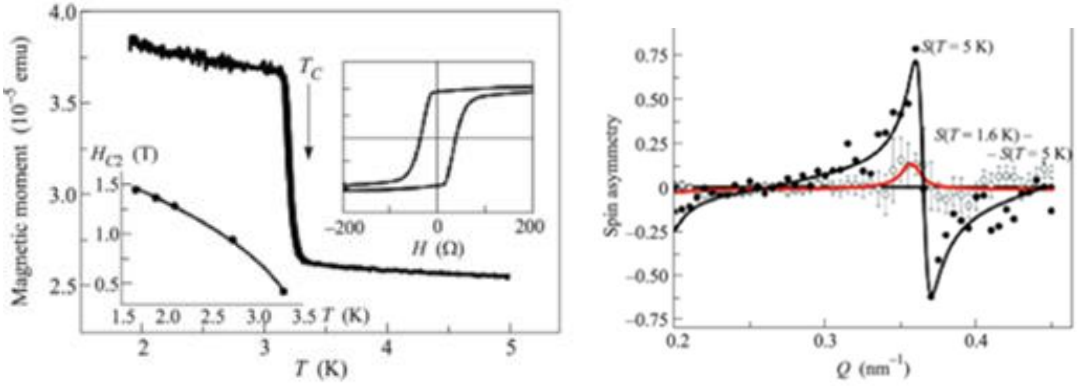

(a) (b)

Fig.4.(a) Temperature dependence of the magnetic moment around TC, measured in magnetic field H = 10 Oe applied parallel to the sample surface. Left inset: temperature dependence of the upper critical field of the S layer (experimental points and their fit shown by the solid line). Right inset: magnetic hysteresis loop measured at T = 10 K.(b) (Points) Experimental and (solid line) model differences of spin asymmetries

In order to define the reason of the increased magnetic moment we have measured the polarized neutron reflectivities above and below Tc in conditions similar to SQUID. The spin asymmetry measured at T = 5 K > Tc is depicted in Fig. 4(b) with the black line. After cooling the sample below Tc the shift of spin asymmetry towards higher Q values was observed near Q = 0.35 nm^{-1}. Such a shift can be described by the appearance in superconducting vanadium of magnetic sublayer with a thickness of 7 nm and a magnetization of +0.8 kG.

Project goals

The aim of this work is to study the coexistence of superconductivity and ferromagnetism in the Nb (100nm) / Gd (3nm) / V (70nm) / Nb (150nm) multilayer structure and make a description of Polarized Neutron Reflectometry at Remur Spectrometer and possibility for secondary radiation registration.

Methods

Description of Polarized Neutron Reflectometry (PNR)

Polarized Neutron Reflectometry has been widely used to study homogeneous and heterogeneous magnetic films, as well as superconductors. Starting from simple profiles, and gradually solving structures of greater complexity, PNR has been used to observe or clarify phenomena as diverse as the magnetism of very thin films, the penetration of fluxoids in superconductors, and the magnetic coupling across non-magnetic spacers [7]. Although PNR is considered to be a probe of depth-dependent magnetic structure, laterally averaged in the plane of

the film, the development of new scattering techniques promises to enable the characterization of lateral magnetic structures.

The wave properties of the neutron make possible the optical study of matter by means of neutron beams. As shown in the figure 5:

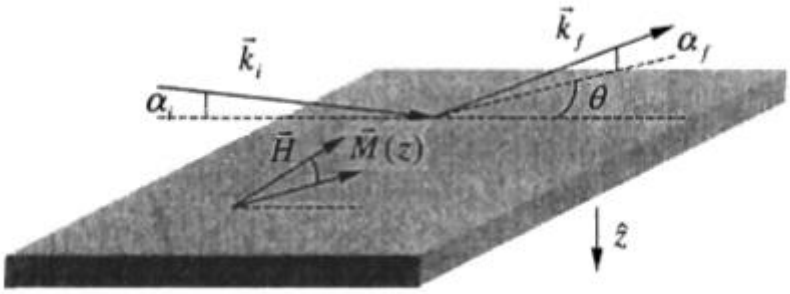

Fig.5. Glancing angles of incidence (α_i) and exit (α_f) characterize experiments done in reflection geometry.

As can be seen, a beam of neutrons is reflected from a flat, laterally homogeneous object. The intensity of the reflected beam, recorded at different neutron wavelengths and angles of incidence, permits an evaluation of the chemical and magnetic depth profile. If the surface is corrugated, or if the material under the surface is no laterally homogeneous, the angle of the exiting neutrons may be different from that of the incoming beam, either in the reflection plane ($\alpha_i \neq \alpha_f$) or out of it ($\theta = 0$), depending on the geometry of the inhomogeneities. The case of specular reflection is the simplest to treat.

For neutrons of thermal energies, the very small angles of incidence can be sufficient to cause the neutrons to be totally reflected from the surface. In general, the reflectivity is unitary for most material up to a value of $Q_c = \sqrt{16\pi Nb}$ of order 0.01A^{-1}. Beyond this limit, the reflectivity decreases rapidly with a mean asymptotic ${Q_z}^{-4}$ dependence.

Neutron reflectometry assumes completely elastic scattering of neutrons:$|\overrightarrow{k_f}| = |\overrightarrow{k_i}| = {2\pi}/{\lambda}$.

$$Q_x = k_{fx} - k_{ix} = {2\pi}/{\lambda}\,(cos\alpha_f - cos\alpha_i)$$

$$Q_z = k_{fz} - k_{iz} = {2\pi}/{\lambda}\,(sin\alpha_f + sin\alpha_i)$$

For specular reflection ($\alpha_i = \alpha_f$): $Q_x = 0$ and $Q_z = 2k_z = {4\pi}/{\lambda}\,sin\alpha$. This is the condition that is used to determine the structure of the material in the z$^-$ direction.

The neutron's momentum $|\vec{k}| = {2\pi}/{\lambda}$can be separated into two components, parallel and perpendicular to the surface. Only the perpendicular ($\hat{z}$) component is altered by the potential describing the laterally homogeneous material. Thus, we can represent the neutron as a particle with kinetic energy $\hbar^2 k_z^2/2m$, hitting a potential of height U(z). If its energy is too low, the neutron bounces back. A part

of the potential, which is present in all matter, is simply related to the scattering length b of the N constituent nuclei per unit volume:U(z)=($\hbar^2$/2m)N(z)b(z). For thermal and cold neutrons, the isotopic b is constant and conveniently tabulated for all nuclei (as well as for the natural isotopic composition of all elements). In free space (above the surface) U(z)≈0, and the neutron wave function is u(z)=exp(ik$_z$ z)+r exp(-ik$_z$ z) for a plane wave incident on the surface from above. The wave function inside the material is linked to the potential by the Schödinger equation, whose solution gives the reflectance r. In a scattering experiment, the observed quantity is the reflectivity R=$|r|^2$. The wave vector transfer Q_z=4π/λ sinθ provides a convenient metric for characterizing the specular reflection process in which incident- and reflected-beam wave vectors (**k$_i$**,**k$_f$**) enter and exit the surface at the same glancing angle α. Since momentum $\hbar Q_z$ is the quantum mechanical conjugate to position z, one can transform the depth profile of scattering material b(z) into reflectivity R(Q_z). The inverse process (from reflectivity to profile) is more complex.

For Q_z>>Q_c, the reflectivity from a sequence of L layers is well described by using the first Born approximation:

$$R \approx \frac{1}{Q_z^4}\left|4\pi \sum_{l=1}[(Nb)_l - (Nb)_{l-1}]\exp(iQ_z d_l)\right|^2$$

Where d_l is the distance of the lth layer's top interface below the surface. Neutron also interacts with the magnetic induction field ***B*** In the presence of magnetic induction, the interaction potential is described by the following expression $U(z) = U_n(z) + U_m(z) = \hbar \mathrm{N(z)b(z)}/2\mathrm{m} + \vec{B}\hat{s}$, where $\hat{s}$ is the neutron spin operator. Since the neutron is a -1/2 spin particle, there are two states of quantization concerning an external magnetic field ***H***. In measurement, the neutron may be polarized either parallel (+) or antiparallel (-) to ***H***. So if we suppose that the neutron is polarized in an applied field ***H$_p$***. Upon encountering and induction ***B$_s$*** with a different orientation (for instance, inside a sample), the neutron changes its spin state. In classical terms, the neutron moment processes about ***B$_s$***. Four reflectivities can be measured R^{++}, R^{+-}, R^{-+}, R^{--}. In the first approximation, the non-spin flip (R^{++}, R^{--}) components determine the component of the magnetic moment parallel to the quantization axis (generally the direction of the external magnetic field) and the spin flip (R^{+-}, R^{-+}) components determine the perpendicular component. The spin-dependent Schödinger equation takes a very simple form when all of the magnetic induction in the neutron path is collinear. In this case, neutrons remain polarized in the original state (R^{+-} = R^{-+} = 0). Neutrons polarized parallel (+) or antiparallel (-) to ***H$_p$*** see potential $U^{\pm} = (\hbar^2/2m)Nb \pm \mu B$, where μ is the neutron magnetic moment. The magnetic medium is, in effect, birefringent. Since the strength of the magnetic scattering in ferromagnetic materials is comparable to that of the nuclear, an analysis of the reflectivities R^{++} and R^{--} makes possible a quantitative determination of *B*(z).

One reflectometer is composed mainly by the components shown in figure 6.

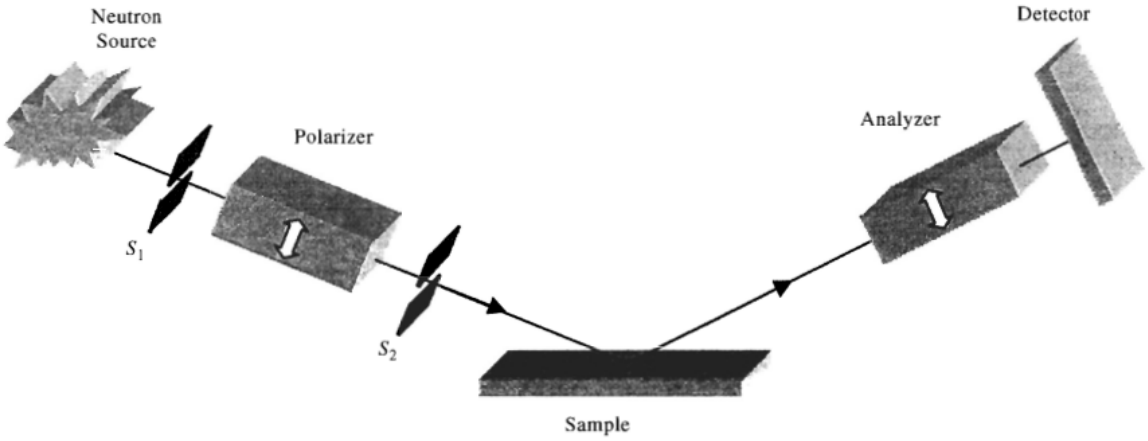

Fig.6. Neutron reflectometers at both fixed-wavelength and broadband sources consist of the same general components: a reactor or spallation neutron source, two slits s_1 and s_2 to define the incident-beam collimation, incident-beam polarizing and spin-flipping elements, a flat sample on a positioning table, exit-beam polarization analysis, and a position-sensitive or single detector.

The instrument functions as a diffractometer with resolution sufficient to separate transmitter and reflected beams at values of Q_z near where the reflectivity becomes unitary. Specular reflectivity ($\alpha_i = \alpha_f$) is solely a function of the momentum transfer along the $\hat{z}$-direction hence in practice a range of Q_z is spanned either by changing the wavelength, and keeping fixed the angle of incidence, or changing the angle of incidence at a fixed wavelength. Appropriate devices, such as polarizing mirrors and flat-coil spin-flippers, polarize the incoming neutrons along an applied magnetic field or analyze the polarization of the reflected beam. Conventionally, the direction of the initial polarization is fixed. The sample may change the neutron's polarization, and an analyzer chooses, among the reflected neutrons, those aligned with the polarizer. Reversal of the neutron spin is obtained by energizing flippers before and after the sample. The reflectivities are then characterized by the neutron polarization sign before and after reflection with respect to the reference field: R^{++}, R^{--}, R^{+-}, and R^{-+}.

Potentiality of PNR

Nuclear Magnetic Resonance (NMR) was used in to detect inverse proximity effect in Ni/V(30–70 nm)/Ni/MgO systems. However, NMR inherently needs the application of DC and AC magnetic fields which makes comparison of the experiment with the theory rather ambiguous. Another article [6] reported upon the observation of the inverse proximity effect in Pb/Ni and Al/CoPd bilayers using the polar magneto-optic Kerr effect. As a requirement of the technique, the authors had to apply a special procedure to magnetize the F layer perpendicular to the sample surface. The above mentioned experimental methods are highly sensitive, but lacking the required depth selectivity. Consequently, the thickness of the induced magnetic sublayer cannot be explored and compared with the theoretical predictions. An alternative experimental method to study the changes in the magnetization state of a sublayer is Polarized Neutron Reflectometry (PNR). Polarized neutron reflectometry measures the nuclear and the magnetic

depth profiles, the latter via the interaction of neutron spins with the magnetic induction in the system. Advantages of the neutrons for such studies are the very low absorption in the layers of the required thickness for superconductivity which allows studying deeply buried S/F interfaces. Another advantage of PNR is the possibility to measure in a low intensity (several Oersteds) and DC–only magnetic fields with arbitrary to the sample plane direction. This allows to avoid problems with data misinterpretation due to the Meissner effect, vortex state etc. To increase magnetic PNR signal, usually multilayered systems are used where the investigated S/F bilayer is repeated several times. Deposition of multilayered S/F structures may inevitably lead to an increased cumulative roughness of the S/F interfaces. Since the magnitude and even the sign of the induced magnetization strongly depends on the quality of S/F interface, this may lead to the situation when induced magnetization is different for the different S/F interfaces. This greatly complicates the interpretation of the PNR data. To enlarge small magnetic scattering in this case waveguide enhancement of the neutron standing waves can be used. The advantage of the method is the strong enhance of the intensity of the magnetic scattering.

Description of Remur Spectrometer and possibility for secondary radiation registration.

In the polarized neutron spectrometer REMUR there is realized:

1. Mode to measure the reflection of polarized neutrons and their transmission through a layered structure (reflectometric mode), and the mode to measure diffuse small-angle neutron scattering (small-angle mode).

2. Complete polarization analysis of the reflected and the scattered neutron beam [12] that allows the investigation of processes with/without a change in the neutron spin state.

3. Polarization analysis of the neutron beam with respect to the local field in the investigated sample based on the effect of spatial splitting of the neutron beam that occurs if there exists a nonzero probability of neutron transition between spin states.

4. Position-sensitive detection of neutrons with the angular resolution in the horizontal plane ±0.17 mrad.

5. Shifting of the polarization efficiency of the reflectometric mode in the neutron wavelength interval 1.5÷5 Å accomplished by changing the glancing angle of the neutron beam falling on the supermirror of the neutron polarizer.

6. Automated switching over of the state of the spectrometer during its operation in a specified mode, automated acquisition of the spectrometric data, control of the state of individual blocks of the spectrometer.

7. Visualization and express-analysis of the spectrometric data.

Figure 7 shows the functional scheme of the spectrometer.

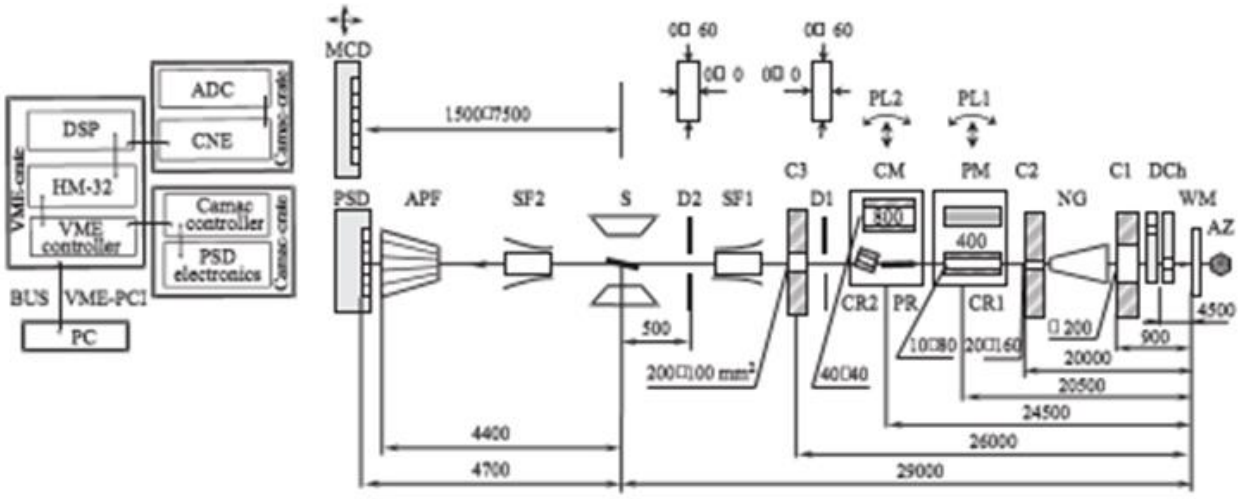

Fig.7.The functional scheme of the REMUR spectrometer: AZ: active zone of the reactor; WM: water moderator; DCh: double disk chopper; C1,C2,C3: collimators; NG: conic neutron guide; PL1,PL2: controlled platforms No.1 and No.2; CR1,CR2: reflectometric collimators; PR: reflectometric polarizer; PM:small-angle polarizer; CM:small-angle collimator; D1,D2: controlled diaphragms; SF1,SF2: spin-flippers; S: sample; APF: focused polarization analyzer; PSD: position-sensitive detector; MCD: small-angle multi-counter detector.

Polarizers and Polarization Analyzer:

The polarizer consists of a super-mirror structure deposited on a glass substrate. The polarizer substrate is produced from a polished piece of glass with a size of 10cm x 80cm x 2.8cm. The critical angle of thermal neutron reflection θ_c (λ =1.8 Å) =6.3 mrad. The principle of operation of the supermirror polarizer (polarization analyzer) consists in that neutrons whose spin projection lies in the direction of the magnetic field (neutrons in '+' spin state) are reflected from the magnetic supermirror layer and neutrons with the spin projection in the opposite to the magnetic field direction (neutrons in '-' spin state) are transmitted through the layer and get absorbed in the next layer that has a larger neutron capture cross section. The neutron beam glancing angle at the polarizer can be adjusted within the limits $3\cdot10^{-3} \div 10^{-2}$ rad by rotating the supermirror, which gives a width of the polarized neutron beam d =0.24 ÷0.8 mm.

The polarization analyzer is performed in the "fan" geometry. The analyzer is a stack of 125 super-mirrors positioned in a magnetic field of a permanent magnet and has an area of window assumed for neutrons with a cross section of 18x20cm^2. Super-mirrors are 0.5 mm-thick glass substrate coated with a m2 type super-mirror coating, characterized by a critical neutron wave vector of 22 mrad/Å (indicated as m2). The mirrors are oriented so as to provide the same glancing angle of the neutron beam on them, equal in this case to 3 mrad.

Spin-Flippers and detectors:

Gradient radio frequency spin flippers, operating at a frequency of 75 kHz are used in the spectrometer. The probability of neutron beam polarization flip $f_1 = f_2$ in the range λ>1.15 Å exceeds 0.99.

Among the advantages of the gradient RF spin-flipper are:

1) A noncollimated neutron beam (divergence up to 0.1 rad) with a large cross section (~100 cm^2).

2) No strong requirements for the stability and homogeneity of the magnetic fields or for the stability of the alternating magnetic field frequency.

3) The absence of substances on the way of the neutron beam.

In the reflectometric mode of the REMUR spectrometer neutrons are registered with a gas-filled one-dimensional position sensitive detector (PSD). PSD is a proportional multiwire cell in a hermetic duraluminium box with a 120 × 40 mm^2 cross-section inlet. The inside dimension of the box is 200 × 100× 48 mm^3. The registration of neutrons is based on the reaction of neutron capture in ^{3}He nuclei and the emission of secondary fission products, protons and tritium nuclei: $^3He(n,p)^3H$ + 764 keV. The gas layer thickness is 24 mm at a ^{3}He pressure of 3.4 atm. To raise the spatial resolution, propane with a partial pressure of 2 atm, is added to the volume of the gas in the detector. The spatial resolution of the detector is 1.5÷2.5 mm (FWHM). The highest resolution, on the order of 1.5 mm, is achieved in the center of the detector. The width of the position channel of the detector is 0.69 mm and the number of position channels is 256. The duration of the time channel is 128 μs and their number is 2048. The dead time of the detector is 37 ns. To perform small-angle scattering experiments with the spectrometer REMUR, a 32-counter detector is used.

Secondary radiation measurement

Neutron reflectometry is a method for measuring the spatial profile of the neutron interaction potential with the medium. The interaction potential is the sum of neutron interaction potentials with separate isotopes of the medium. To determine the neutron interaction potential with the structure units, secondary radiation is simultaneously registered with neutrons. Channels for registering secondary radiation of charged particles, gamma rays and neutrons, having experienced spin flip, have been developed on the REMUR spectrometer of the IBR-2 reactor in Dubna (Russia).

At the interface between two media, the interaction potential is the sum of interaction potentials of elements penetrating each other. In this regard, standard neutron reflectometry does not allow one to identify to what kind of elements the changes of the interaction potential and, in particular, of the magnetic profile, are related. For defining the potential profile of the neutron interaction with separate elements, it is necessary to register secondary radiation from isotopes of elements. The type of radiation and the radiation energy are the signs identifying isotopes of elements. Charged particles, gamma rays and nuclear fission fragments are considered as secondary radiation. In a broader interpretation,

secondary radiation should include neutrons, incoherently scattered at nuclei, neutrons inelastically scattered by atoms and the medium, as well as diffusely scattered neutrons at interfaces and inhomogeneities in the layers of the structure. The signs of such secondary radiation are the angular distribution and the transfer energy of scattered neutrons. The particular secondary radiation includes neutrons having experienced a coherent spin flip in a noncollinear magnetic structure. In this case, at neutron propagation, neutrons are “absorbed” in the initial spin state and, correspondingly, neutrons occur in final spin state. For determining the spatial distribution of elements and increasing the sensitivity of measurements, neutron standing wave regime are used.

Channels for recording of the secondary radiation are created at spectrometer polarized neutrons REMUR located at IBR-2 pulsed reactor in Dubna (Russia). IBR-2 reactor operates with a frequency of 5 Hz. Spectrometer REMUR has next basic parameters: distance from sample place to the moderator is 29 meters, distance from the sample place to neutron detector is 5 meters, the wavelength resolution at detector place is $\delta\lambda$=0.02 Å.

Channel of charged particles: The main unit of the channel is the ionization chamber installed in the goniometer of the sample module. A neutron beam enters the chamber through the input window and falls on the structure mounted on the cathode of the chamber. The reflected and refracted on structure neutron beams exit the chamber through the output window and are registered using a position-sensitive detector positioned at a distance of 4.9 m from the chamber. The scattering intensity of neutrons does not exceed 0.5% during their passage through the chamber windows. To adjust the glancing angle of the neutron beam to the plane of the structure, the ionization chamber is oriented by turning around the vertical axis in the range of 1–10 mrad with an accuracy of 0.1 mrad. Inside of the ionization chamber is placed investigated layered structures. Layered structures included neutron absorption layers $^{6}Li_{0.9}{}^{7}Li0.1F$(5 nm). The ORTEC 142A charge-sensitive preamplifiers are directly installed on the ionization chamber, to which registration signals of a charged particle are supplied from the cathode and anode of the chamber.

Channel of gamma rays. To register gamma rays, a semiconductor germanium detector operating in the range of 3 keV - 10 MeV can be used. The germanium crystal has a diameter of 61.2 mm and a length of 87.3 mm. For gamma radiation with an energy of 1.33 Mev, the registration efficiency is 45%, the energy resolution was 2 keV.

In real time at the neutron spectrometer REMUR enough many isotopes are available for measurements with registration of secondary radiation. Further progress is connected with increasing of neutron intensity in 10 times, decreasing of the background of fast neutrons and gamma radiation from active reactor zone in 4-10 times, increasing of gamma detector solid angle in 4-5 times. Together using of these measures will allows to reach $\sigma_{min}\approx$1 mbarn at h=5 nm or h$\approx$1 Å at σ_{min} =50 mbarn. With supermirror reflector can be achieved a spatial resolution of 1 Å also.

Results

In this work have been studied magnetic properties of the structure Nb(100nm)/Gd (3nm) / V (70nm) / Nb (150nm).

For most S/F heterostructures composed of elemental metals or alloys, T_F greatly exceeds T_c. In such systems, one expects significant magnetic proximity effects if the effective energy $E_F \sim T_F d_F/d_S$ becomes comparable to $E_S \sim T_c$, where d_F (d_S) are the thicknesses of the F (S) layers [2]. Gadolinium is a weak ferromagnet with T_F =293 K, which, in combination with Nb, the strongest elemental superconductor with T_c = 9.3 K, allows for the preparation of S/F systems with $E_F \sim E_S$.

In order to process the experimental data these were displayed through Spectraviewer software. Then, in order to model the phenomena, a software, coded in Matlab, based on the Schrodinger equation results for this problem, was used. And at last, was used Origin Software to make graphs.

Neutron measurements were conducted in Dubna using a polarized neutron time-of-flight spectrometer REMUR of the IBR-2 reactor. To change the polarization of a beam incident on a sample a spin flipper was used, when a spin flipper was switched off (on) the intensity of scattered neutrons with “+” (“–”) polarization was measured, where the sign indicates the neutron projection on the external magnetic field.

In order to make experimental measurements the following protocol was used: first the structure (Nb (100nm) / Gd (3nm) / V (70nm) / Nb (150nm)) was cooled down to T=12K at H=20 Oe Later the external magnetic field was increased to a value of H=1.9 Oe and this value was sustained for one minute. After that, the external magnetic field’s intensity decreased to H=500 Oe at 12K and the data was collected under these conditions. At last, the system’s temperature decreased from 12K to 1.5K and a set of measurements were performed at T=1.5K, H=500 Oe.

The spin-up and spin-down specular neutron reflectivities $R^+(\lambda)$ and $R^-(\lambda)$ as a function of the wavelength λ were measured using position sensitive detectors (PSD). Since the magnetic contribution to the neutron scattering is small, it is useful to single it out using the so-called spin asymmetry:

$$S(\lambda) = [R^+(\lambda) - R^-(\lambda)]/[R^+(\lambda) + R^-(\lambda)].$$

In the following graph we compare the behavior of spin asymmetry at 12 and 1.5 K.

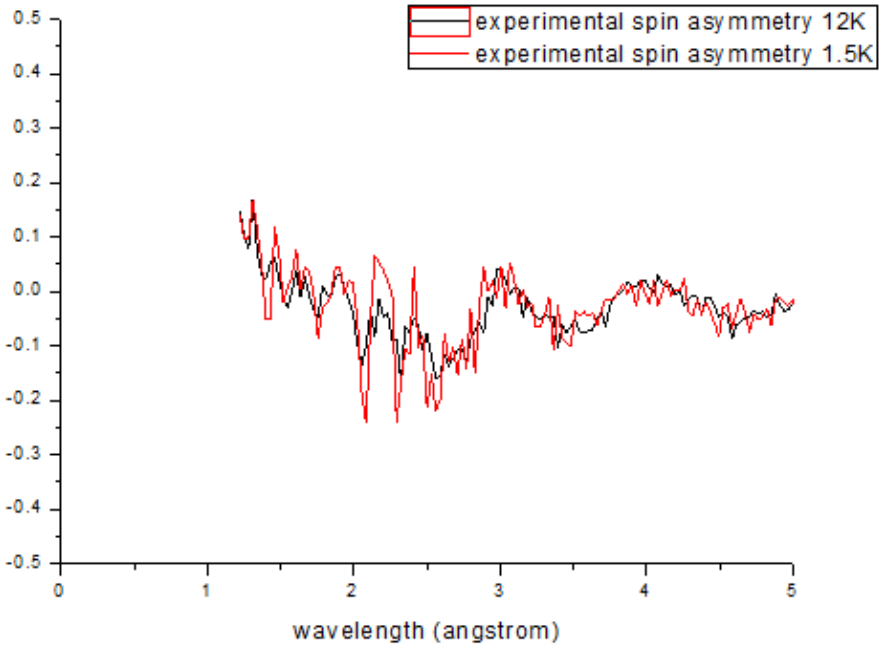

Fig.8. Experimental spin asymmetry as function of wavelength at 12 and 1.5 K.

As can be seen (for both curves) in the range (1.7-2.6 Å) spin asymmetry oscillates near to zero with period $T_\lambda \approx 0.3$ Å, which corresponds to $T_Q \approx 0.29$ Å^{-1}. And realize another oscillation near to zero in (2.6-3.5 Å).

The module of spin asymmetry at 1.5 K, in general, is bigger than it is at 12 K for a same wavelength. It means that the dependence of the magnetization on the wavelength is more pronounced at (T<Tc) than at (T>Tc).

In order to plot theoretic spin asymmetry, let's to consider two models. In the first one, we are going to suppose that the magnetization of the ferromagnetic layer at 12 K is bigger than it is at 1.5 K. In the second model, we are going to suppose the opposite that means that the magnetization of the ferromagnetic layer at 12 K is larger than it is at 1.5 K. In the case of coming true the first model we would be talking about the possible appearing of a diamagnetic moment in the superconductor opposed to the external magnetic field and as a result decreases the magnetization of the ferromagnet. The second model would imply the appearing of a paramagnetic magnetization that contributes to the increase of the magnetization in the ferromagnet.

The following figure shows a comparison of both models with the experimental obtained results to spin asymmetry at T=12 K.

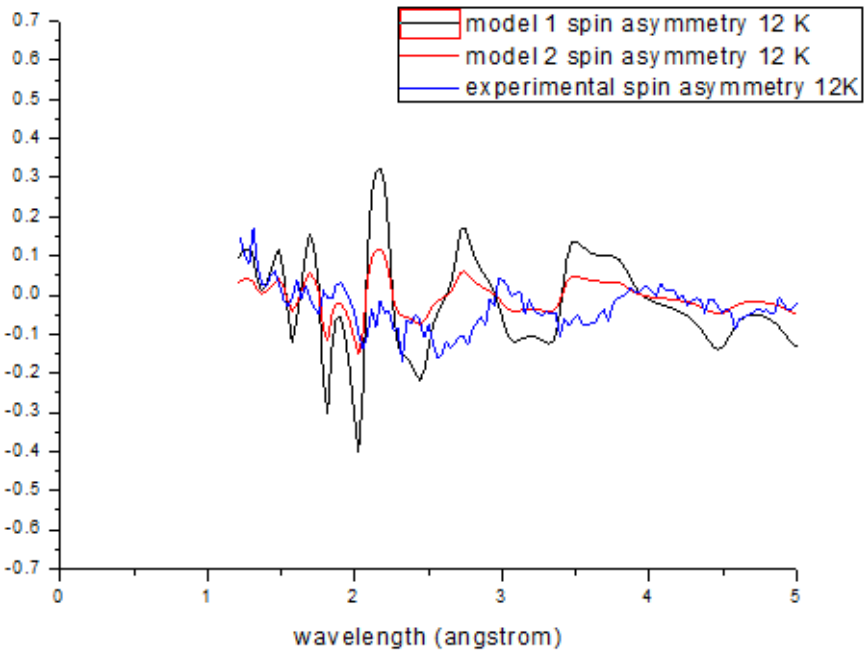

Fig.9. Comparison between model 1, model 2 and experimental spin asymmetry as function of wavelength at 12 K.

As can be seen model 2 fits better to the experimental curve.

The following figure depicts comparison between model and experimental spin asymmetry as function of wavelength at 12 and 1.5 K.

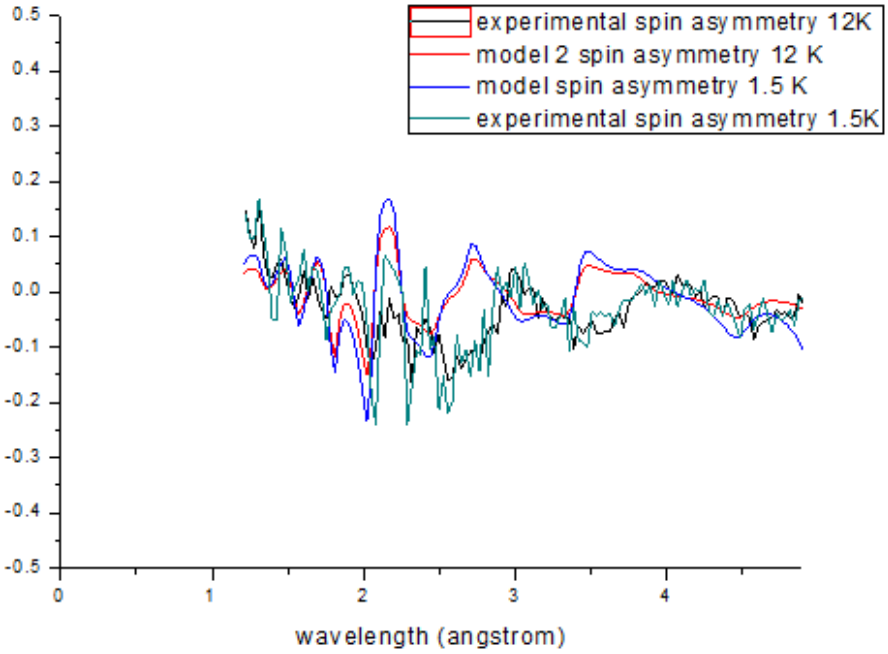

Fig.10. Comparison between theoretic and experimental spin asymmetry as function of wavelength at 12 and 1.5 K.

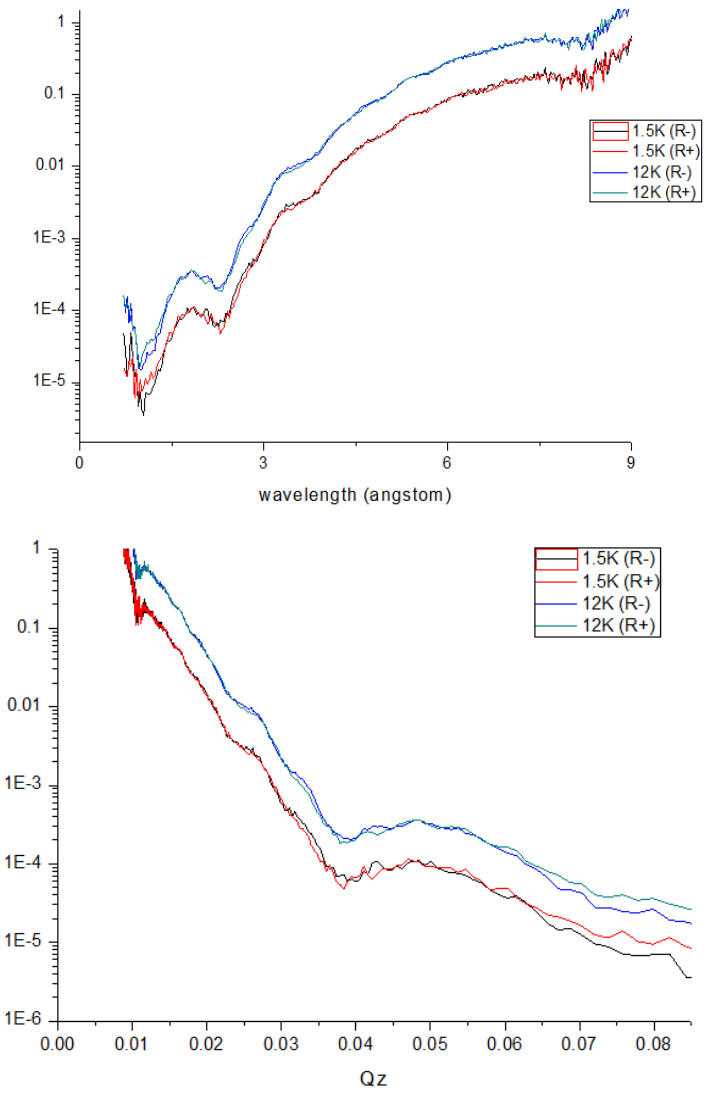

Fig.11

Figure 11 compare reflectivity as a function of the wavelength (λ) and the transferred vector (Q_z) for spin-up and spin-down for 12K and 5 K. As can be seen for one same value of wavelength, reflectivity is bigger at 12K (T>Tc) than at 1.5K (T<Tc) it means that a bigger number of neutrons are reflected at T>Tc than at (T<Tc) and other processes are more likely (e.g neutrons transmission) at (T<Tc) than at (T<Tc). As can be seen in the figure there is a peak at λ≈1.8 Å (Q≈ 0.049$Å^{-1}$), by increasing wavelength can be orserved and incresase in reflectivity until 1 as it was expected to happen.

Conclusion

In this work have been studied magnetic properties of the structure (100nm) Gd (3nm) V (70nm) Nb (150nm)) (Nb. We compared the experimental curve of spin asymmetry with the theoretician based on two different models. The spin-up and spin-down experimental curves were performed at 1.5 y 12K. Inverse proximity effect takes place through the magnetization of the superconductor because of the action of the ferromagnet over it.

Acknowledgements

I would like to thank to Joint Institute for Nuclear Research (JNIR), especially to my supervisor Vladimir Zhaketov who gave me the opportunity to be part of this remote training course and guided me through it. I would like to thank to the team that was in charge of performing measurements, which associated

collected data used in this project. This work is based on experiments performed at Dubna using the spectrometer REMUR of the IBR-2 reactor.

References

1- “Electromagnetic proximity effect in planar superconductor-ferromagnetic structures”. S. Mironov, A. S. Mel’nikov and A. Buzdin.

2- “Magnetic proximity effect in Nb/Gd superlattices seen by neutron reflectometry”. Yu. N. Khaydukov, E.A. Kravtsov, V. D. Zhaketov, V. V. Progliado, G. Kim, Yu. V. Nikitenko, T. Keller, V. V. Ustinov, V. L. Aksenov, and B. Keimer.

3- “On the Feasibility to Study Inverse Proximity Effect in a Single S/F Bilayer by Polarized Neutron Reflectometry”. Yu. N. Khaydukov, B. Nagy, J.H. Kim, T. Keller, A. Rühm, Yu. V. Nikitenko, K. N. Zhernenkov, J. Stahn, L. F. Kiss, A. Csik, L. Bottyán, and V. L. Aksenov.

4- “Magnetism in Structures with Ferromagnetic and Superconducting Layers”. V. D.Zhaketov a , Yu. V. Nikitenko, F. Radu, A. V. Petrenko, A. Csik, M. M. Borisov, E. Kh. Mukhamedzhanov, and V. L. Aksenov.

5- “Coexistence of Superconductivity and Ferromagnetism in the Nb(500 Å)/Fe(39 Å)[Si(34 Å)/Mo(34 Å)]$_{40}$/Si Nanostructure”. V. L. Aksenov, Yu. V. Nikitenko, Yu. N. Khaidukov, S. N. Vdovichev, M. M. Borisov, A. N. Morkovin and E. Kh. Mukhamedzhanov.

6- “Inverse Proximity Effect in Superconductor-Ferromagnet Bilayer Structures”. J. Xia, V. Shelukhin, M. Karpovski, A. Kapitulnik and A. Palevski.

7- “Polarized Neutron Reflectometry”. J.F. Ankner and G.P Felcher.

8- “Neutron Reflectometry: A probe for materials surfaces”. J. Penfold, Z. Tun, R. Cubitt, J. J. Cubitt, A. R. Rennie, A. Nelson, M. James, J. C. Schulz, A. Brule, K. Mergia, G. Apostolopoulos, L. Cser, S. Basu, S. Singh, A. R. Wildes, A. Ruhm, U. Wildgruber, J. Franke, J. Major, H. Dosch, H. Leeb.

9- “The polarized Neutron Spectrometer REMUR at the pulsed Reactor IBR-2”. V. L. Aksenov, K. N. Jernenkov, S. V. Kozhevnikov, H. Lauter, V. Lauter-Pasyuk, Yu. V. Nikitenko, A. V. Petrenko.

10- “Neutron reflectometry with registration of secondary radiation”. V. D. Zhaketov, A. Petrenko, Yu. M. Gledenov, Yu. N. Kopatch, N. A. Gundorin, Yu. V. Nikitenko, V. L. Aksenov.

11- “Reflectometry with registration of secondary radiation at local neutron reflection”. V. D. Zhaketov, A. Petrenko, Yu. N. Kopatch, N. A. Gundorin, C. Hramko, Yu. M. Gledenov, Yu. V. Nikitenko, V. L. Aksenov.